JOURNAL OF MATERIALS SCIENCE **34** (1999) 5497–5503

Thermal conductivity of graded composites: Numerical simulations and an effective medium approximation

P. M. HUI
Department of Physics, The Chinese University of Hong Kong, Shatin, New Territories, Hong Kong

X. ZHANG*
Department of Physics, The Ohio State University, Columbus, OH 43210-1106, USA

A. J. MARKWORTH
Department of Materials Science and Engineering, The Ohio State University, Columbus, Ohio, 43210-1179, USA

D. STROUD
Department of Physics, The Ohio State University, Columbus, OH 43210-1106, USA
E-mail: stroud@ohstpy.mps.ohio-state.edu

We describe two methods for modeling the thermal conductivity and temperature profile in a graded composite film. The film consists of a random binary composite, whose concentration varies in the direction perpendicular to the film surface, and a fixed temperature difference is applied across the film. In the first method, the temperature profile is modeled directly, using a finite element technique in which the film is represented as a discrete network of thermal conductances, randomly distributed according to the assumed composition profile. The temperature at each node, and the effective thermal conductance, is then obtained by a transfer matrix technique. In the second approach, the film is treated by an effective-medium approximation, suitably generalized to account for the composition gradient. The methods are in rough agreement with each other, and suggest that thermophysical properties of the film can be treated reasonably well by approaches generalized from those which succeed in conventional composites.

1. Introduction

Spatially graded composites are materials comprised of two or more phases, in which the average composition varies along some spatial direction. Such materials have a variety of applications. For example, they form excellent thermal barriers for separating a region of high temperature from one of lower temperature. In such an application, a metal/ceramic composite would be appropriate. The high-temperature side would be predominantly ceramic in order to maintain the required mechanical integrity, while the low-temperature side would be predominantly metallic in order to produce desirable mechanical and heat-transfer characteristics. It has been pointed out by Hirai [1] that most naturally occurring materials (e.g., bamboo) are functionally graded, having continuous variation of composition and structure. The development of models for functionally graded composites, for use in design of optimal microstructures, has received considerable attention over the past several years [1, 2]. These models require, in turn, knowledge of the manner in which relevant thermophysical properties vary with spatial position as a result of compositional variations.

In the present paper, we address the problem of modeling the thermophysical properties of graded composites using two different approaches, and apply the results to the calculation of thermal conductivity of spatially graded composites. This property is of great importance, for example, in applications of metal/ceramic graded composites for use as thermal barriers. Our first approach is a direct numerical simulation of the thermal conductivity and temperature distribution in such a composite, using a finite-element method in which the composite is represented by a discrete network. The required temperature distribution and effective thermal conductivities are then obtained by a transfer matrix algorithm. In the second approach, we derive the same properties using an extension of a well-known effective-medium approximation (EMA). While this second approach is not as accurate as a direct simulation, it gives

* *Present address*: *Qwest Communications, 6000 Parkwood Pl., Dublin, OH 43017, USA.*

results qualitatively similar to the exact numerical solutions. Because of this similarity, and its analytical ease of execution, this approximation is likely to be useful in obtaining quick and reasonable estimates of thermal profiles and effective conductivities for a wide range of graded composites.

We turn now to the body of the paper. Section 2 describes the general model used to describe the graded composites. In Section 3, we describe our numerical method of solution for the temperature profile, and present some numerical results for various methods of grading the concentration. In Section 4, we present the corresponding EMA for such graded materials, display the solutions for a variety of concentration profiles, and compare the results with the numerical solutions in several cases. A discussion, and suggestions for further applications, follow in Section 5.

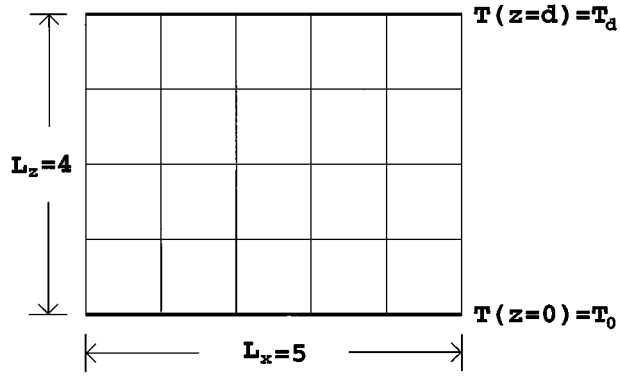

Figure 1 Schematic of the geometry used to calculate the effective thermal conductivity $\kappa_{e,\perp}$ and temperature profile $T(z)$ using the transfer matrix algorithm. In this sketch, the film lies between $z = 0$ and $z = d$, with the two sides being fixed at temperatures T_0 and T_d ($T_d > T_0$). The concentration p of poor conductor varies in the z direction and is larger at $z = d$ than at $z = 0$. The effective thermal conductivity and temperature profile of the film are calculated using the transfer matrix algorithm, as described in the text.

2. Model

Our model for the functionally graded composite (FGC) is quite simple. We take the composite to be a thin film made up of two components, a poor thermal conductor and a good thermal conductor. The concentration of bad conductor is denoted $p(z)$, which we assume to vary only in the z direction, i.e., perpendicular to the film, as is characteristic of an FGC. We take the two faces of the film to lie at $z = 0$ and $z = d$, where d is the film thickness. We assume that $p(z = 0) = p_0$ and $p(z = d) = p_1$, with $p_1 \geq p_0$, corresponding to a higher concentration of good conductor at the bottom ($z = 0$) and poor conductor at the top of the film ($z = d$). Within the film, we consider various models for the variation of $p(z)$. The film can then be described by effective thermal conductivities $\kappa_{e,\perp}$ and $\kappa_{e,\parallel}$ perpendicular and parallel to the film. For this anisotropic geometry, these will, in general, be different, even if the thermal conductivities κ_1 and κ_2 of the components are scalars. Usually we assume boundary conditions consistent with the typical use of these films: $T(z = 0) = T_0$ and $T(z = d) = T_d$, with $T_d \geq T_0$. In this geometry, the film acts as a shield which protects a colder substrate from a hotter environment.

Both of the methods to be described below allow one to calculate not only $\kappa_{e,\perp}$ and $\kappa_{e,\parallel}$, but also the temperature profile within the film. In the next sections, we outline the two methods, as well as our results as obtained from each method.

3. Finite-element simulation

3.1. Description of the method

In the finite-element approach, one represents the film as a discrete network of thermal conductances. Specifically, the network is a mesh of points on a simple cubic lattice; the bonds are chosen at random to be bad conductor with conductance κ_1 or good conductor with conductance κ_2 with probabilities $p(z)$ and $1 - p(z)$ respectively. (The z coordinate of bonds parallel to the z axis is taken as that of the midpoint.) We then solve the Kirchhoff equations for the heat conduction on this lattice numerically. The output includes the effective thermal conductivities $\kappa_{e,\parallel}$ and $\kappa_{e,\perp}$ parallel and perpendicular to the films. The same technique allows us to calculate the average temperature gradient in each layer, or equivalently, the average thermal conductivity of each layer in the z direction. We can use any desired model for $p(z)$, as well as various meshes of different fineness. This latter freedom may give information about the importance of the ratio of particle size to film thickness, in determining $\kappa_{e,\parallel}$ and $\kappa_{e,\perp}$.

In order to calculate $\kappa_{e,\parallel}$ and $\kappa_{e,\perp}$ for this geometry, as well as to calculate the local thermal gradients within the composite, we use a transfer matrix algorithm which has proven to be very successful for the analogous problem of calculating the electrical conductivity and local electric field of an inhomogeneous conducting film. The problems are mathematically equivalent, though of course physically very different. The method was first developed to calculate the electrical conductivity by Derrida and Vannimenus [3], and was generalized to allow for calculation of electric field distribution within a random network by Duering *et al* [4]. These methods have already been applied to a range of linear and nonlinear electrical problems in composite materials (see, for example, [5, 6]). Both methods provide a very efficient method of solving the analog of the Kirchhoff circuit equations for these networks, which have the special kind of random distribution described above. The geometry used for the transfer matrix calculation is shown schematically in Fig. 1.

3.2. Numerical results

Table I shows the average temperature profile $T(z)$ as a function of z in the simplest graded composite, in which the concentration $p(z)$ varies linearly with z ($p(z) = z/d$). In this case, we have assumed that the ratio κ_2/κ_1 of good to bad conductivities is 100. Table II shows the effective conductivities $\kappa_{e,\perp}$ in the direction perpendicular to the film for two different concentration profiles: $p(z) = z/d$, and $p(z) = 1 - [(1 - z/d)^2]$. In both cases, the calculation is carried out for a

TABLE I Average temperature $T(z)$ at as a function of normalized distance z into film, as calculated numerically using the transfer matrix approach.The grid (as described in the text) is $10 \times 10 \times 100$. The concentration of bad thermal conductor is assumed to be $p(z) = z/d$. The boundary conditions are $T(z = 0) = 0$, $T(z = d) = 1$. The ratio κ_2/κ_1 of good of bad conductances is 100

z/d	T
1.0	1
0.9	0.22164
0.8	0.17132
0.7	0.13750
0.6	0.11392
0.5	0.09016
0.4	0.07083
0.3	0.05188
0.2	0.03341
0.1	0.01495
0.0	0

TABLE II Effective thermal conductivity $\kappa_{e,\perp}$ in the direction perpendicular to the film, plotted as a function of fineness of grid, for an $L \times L \times 100$ sample and two different variations $p(z)$ of concentration of bad conductor. The ratio of good to bad bond conductances is $\kappa_2/\kappa_1 = 100$, and the concentration of bad conductor is $p(z) = z/d$ (column 2), and $p(z) = 1 - (1 - z/d)^2$ (column 3)

L	$\kappa_{e,\perp}/\kappa_1$ $[p = z/d]$	$\kappa_{e,\perp}/\kappa_1$ $[p = 1 - (1 - (z/d))^2]$
20	3.5968	2.0798
40	3.6396	2.0648
60	3.669	2.0706
80	3.6672	2.0736
100	3.685	2.08

TABLE III Same as Table II, except that we plot the effective thermal conductivity $\kappa_{e,\parallel}$ in the direction parallel to the film, with $p(z) = z/d$. In this calculation the sample size is $L \times 10 \times$ 10,000

L	$\kappa_{e,\parallel}/\kappa_1$
2	50.5504
3	42.5116
4	40.1005
5	39.1900
6	38.5724

$L \times L \times 100$ slab of points (in the sense described in [6]). If one views the length of a bond as a crude measure of the grain size in the composite, then the size dependence of the results might be interpreted as an indication of the importance of grain size, relative to film thickness, in determining the thermal properties of the composite. Table III is a tabulation of the conductivity $\kappa_{e,\parallel}$ in the direction parallel to the film, for a linear concentration profile, once again shown as a function of mesh fineness L.

4. Effective medium approximation

4.1. Formalism

Next, we discuss a simple quasi-analytical approximation which reproduces some of the numerical results which were obtained in the previous sections using discrete network models.

We consider the graded composite of the previous section, containing a volume fractions $p(z)$ and $1 - p(z)$ of materials with thermal conductivities κ_1 and $\kappa_2(\kappa_2 > \kappa_1)$, distributed at random. To achieve the purpose of an FGM, $p(z)$ is chosen in such a way that there is a higher concentration of good conductor near the bottom of the film. Since the bottom of the film (at $z = 0$) is maintained at a temperature T_0 and the top (at $z = d$) at temperature $T_d \geq T_0$, an average temperature gradient of $(T_d - T_0)/d$ is created across the entire film. The problem is to develop a theory to estimate the temperature profile and the effective thermal response.

Note that while $p(z)$ may vary smoothly, the effective thermal conductivity $\kappa(z)$, which describes the *local* in-plane thermal conductivity of a particular layer located at z, may have a different variation, since $\kappa(z)$ depends sensitively on $p(z)$. In particular, for a slab of material at z, if the concentration of the good thermal conductor $(1 - p(z))$ exceeds a critical value p_c, then that slab has a large thermal conductivity $\kappa(z)$, whereas, if $(1 - p(z)) < p_c$, then $\kappa(z)$ is small. Thus, a linear variation of concentration $p(z)$ varying from $p = 0$ to $p = 1$ over the film thickness will not produce a linearly varying $\kappa(z)$. Instead, the entire region where $1 - p(z) < p_c$ has a low thermal conductivity. This *percolation effect* depends on the percolation threshold p_c for the high-conductivity component. This percolation effect must be properly included in considering the thermal response of the FGM; it is included in both the numerical simulations given above, and the analytical approximation which we now describe.

The EMA theory to be presented consists basically of two ingredients. First, $\kappa(z)$ is found by using the three dimensional (3D) Bruggeman effective medium approximation (EMA). The 3D EMA is appropriate here because, although we are interested in the thermal conductivity of a given layer, the current can also be transported in the direction perpendicular to the film plane. The temperature profile $T(z)$ perpendicular to the film thickness is then obtained by solving a one-dimensional (1D) boundary value problem in the z-direction. This approach provides a simple theory for estimating the properties of the FGM.

4.1.1. EMA for $\kappa(z)$

Since the equations governing steady state problem in heat conduction are analogous to those for electrical transport, we can readily extend the electrical EMA to determine $\kappa(z)$. Explicitly, the thermal equations in the steady-state are $J_Q = -\kappa \nabla T$ and $\nabla \cdot J_Q = 0$, where J_Q is the heat current density, while in the analogous electrical transport problem, the equations are $J = -\sigma \nabla V$ and $\nabla \cdot J = 0$, where J is the electrical current density, V the electrostatic potential, and σ the electrical conductivity. The EMA in 3D is a quadratic equation for the local thermal conductivity which takes the form [7]

$$p(z)\frac{\kappa_1 - \kappa(z)}{\kappa_1 + 2\kappa(z)} + (1 - p(z))\frac{\kappa_2 - \kappa(z)}{\kappa_2 + 2\kappa(z)} = 0. \quad (1)$$

The positive solution to Equation 1 for $\kappa(z)$ is

$$\frac{\kappa(z)}{\kappa_1} = \frac{1}{4}\left[(1-3p(z))\left(\frac{\kappa_2}{\kappa_1}-1\right)+\frac{\kappa_2}{\kappa_1}\right] + \frac{1}{4}\sqrt{\left[(1-3p(z))\left(\frac{\kappa_2}{\kappa_1}-1\right)+\frac{\kappa_2}{\kappa_1}\right]^2+8\frac{\kappa_2}{\kappa_1}}. \quad (2)$$

For any given concentration profile $p(z)$, Equation 2 gives the local thermal conductivity $\kappa(z)$.

4.1.2. Temperature Profile

Once $\kappa(z)$ is known, the problem reduces to a 1D boundary value problem along the z-direction. The steady state equation is

$$\frac{d}{dz}\left[\kappa(z)\frac{dT(z)}{dz}\right] = 0, \quad (3)$$

with boundary conditions $T(z=0)=T_0$; $T(z=d)=T_d$. Equation 3 can be formally integrated to give

$$T(z) = T_0 + A\int_0^z \frac{1}{\kappa(z')}\,dz', \quad (4)$$

where A is determined by $T(d)=T_d$. Together with Equation 2 for $\kappa(z)$, Equation 4 gives a simple expression for determining $T(z)$ across the entire film.

One may define an effective thermal conductivity $\kappa_{e,\perp}$ for the entire film via its inverse, by averaging $1/\kappa(z)$ over the film thickness, i.e.,

$$\frac{1}{\kappa_{e,\perp}} = \frac{1}{d}\int_0^d \frac{1}{\kappa(z')}\,dz'. \quad (5)$$

(The inverse is averaged because, in calculating $\kappa_{e,\perp}$, the thermal *resistances* of the layers add in series.) Using Equation 5, Equation 4 for $T(z)$ can be re-expressed in terms of the effective thermal conductivity as

$$T(z) = T_0 + \frac{T_d - T_0}{d}\kappa_{e,\perp}\int_0^z \frac{1}{\kappa(z')}\,dz'. \quad (6)$$

Equations 2, 5 and 6 are the main results of the present theory. For any given concentration profile, they can be applied to estimate the temperature profile and the effective thermal response. Conversely, they can be used to find the optimum concentration profile needed to produce a specific temperature profile desired for a particular application. For an arbitrary concentration profile, $T(z)$ can be easily obtained by numerical integrating Equation 4, or equivalently Equation 6, and using the appropriate boundary conditions.

Similarly, the effective thermal conductivity $\kappa_{e,\parallel}$ in the direction parallel to the film can be defined within the EMA as

$$\kappa_{e,\parallel} = \frac{1}{d}\int_0^d \kappa(z)\,dz. \quad (7)$$

4.2. Applications

4.2.1. Linear concentration profile

As a first illustration, we consider a linear concentration profile across the thickness of the film. A special case of a linear profile is $p(z) = z/d$, so that $p(z)$ varies from $p=0$ at the bottom of the film ($z=0$) to $p=1$ at the top of the film ($z=d$). In this case, the local thermal conductivity following from Equation 2 is

$$\frac{\kappa(z)}{\kappa_1} = \frac{1}{4}\left[\left(1-3\frac{z}{d}\right)(\beta-1)+\beta\right] + \frac{1}{4}\sqrt{\left[\left(1-3\frac{z}{d}\right)(\beta-1)+\beta\right]^2+8\beta}, \quad (8)$$

where $\beta \equiv \kappa_2/\kappa_1$ is the ratio of the thermal conductivities of the two components. The spatial variation of $\kappa(z)$ for this concentration profile is shown in the inset of Fig. 2 for $\beta = 100$, corresponding to the case studied numerically in the previous section; the percolation effect is clearly evident.

The temperature profile for this linear concentration profile can be calculated analytically. Substituting Equation 8 into Equation 4 and defining the dimensionless quantity $x = (1-3z/d)(\beta-1)+\beta$, so that $2-\beta < x < 2\beta-1$ for the allowed range of z, the integral for $T(z)$ can be cast into the form

$$T(z) = -\frac{4A}{3(\beta-1)}\int \frac{1}{x+\sqrt{x^2+8\beta}}\,dx. \quad (9)$$

The integration can be carried out to give

$$T(x) = \frac{-4A}{3(\beta-1)}\left\{-\frac{x^2}{16\beta}+\frac{x}{16\beta}\sqrt{x^2+8\beta} + \frac{1}{2}\ln\left(x+\sqrt{x^2+8\beta}\right)\right\}+B, \quad (10)$$

where the constants A and B are determined by the boundary conditions. Upon solving for A and B, we finally obtain

$$T(x) = T_d - \frac{T_d-T_0}{C}\left\{-\frac{x^2}{16\beta}+\frac{x}{16\beta}\sqrt{x^2+8\beta} + \frac{1}{2}\ln\left(\frac{x+\sqrt{x^2+8\beta}}{4}\right)+\frac{\beta-2}{8}\right\}, \quad (11)$$

where the denominator C is given by

$$C = \frac{1}{2}\ln\beta + \frac{\beta^2-1}{8\beta}. \quad (12)$$

TABLE IV Temperature profile for different concentration profiles, as obtained using the effective-medium approximation. Effective conductivity perpendicular to the film for these profiles is shown in the bottom line of the Table

z/d	$p(z) = z/d$	$(z/d)^2$	$(z/d)^{1/2}$	$(1 + 3(z/d)^2)/4$	$(3/4)\sqrt{z/d}$	$1 - [1 - (z/d)]^2$
1	1	1	1	1	1	1
0.9	0.57104	0.36517	0.72250	0.48808	0.67557	0.75979
0.8	0.28495	0.14217	0.49066	0.21948	0.45299	0.53368
0.7	0.13125	0.09064	0.30657	0.12043	0.30862	0.33564
0.6	0.07071	0.06700	0.17204	0.08315	0.21443	0.17920
0.5	0.04518	0.05101	0.08690	0.06148	0.14959	0.07623
0.4	0.03028	0.03841	0.04326	0.04560	0.10234	0.02935
0.3	0.01987	0.02765	0.02270	0.03253	0.06643	0.01394
0.2	0.01189	0.01795	0.01146	0.02100	0.03846	0.00701
0.1	0.00543	0.00884	0.00445	0.01031	0.01653	0.00285
0	0	0	0	0	0	0
$\kappa_{e,\perp}$	5.01644	8.79267	2.99639	6.47546	12.5329	2.42561

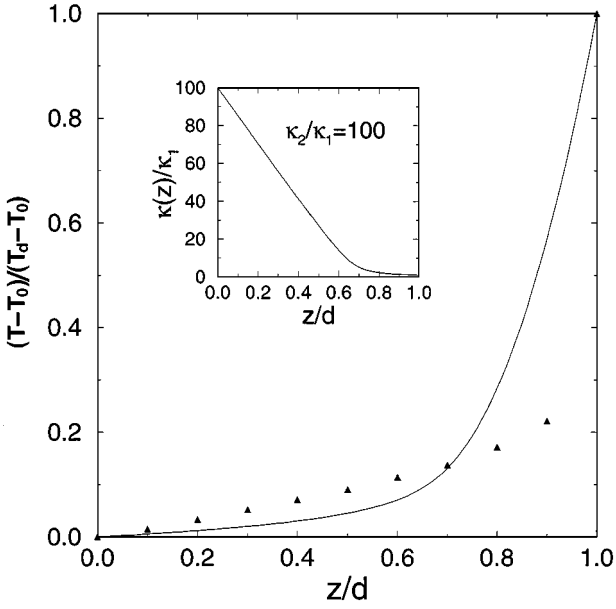

Figure 2 Plot of the temperature profile $T(z)$ within a functionally graded composite film in which the concentration $p(z)$ of poor conductor varies linearly from 0 at the bottom of the film (at $z = 0$) to 1 at the top of the film (at $z = d$). The boundary conditions are $T(z = 0) = T_0$; $T(d) = T_d$. Full line: EMA [Equation 11]; points, numerical simulations. In both cases, we assume $\beta \equiv \kappa_2/\kappa_1 = 100$. The inset shows the local thermal conductivity $\kappa(z)/\kappa_1$ as function of the position z/d as calculated within EMA [Equation 8]. Both the temperature profile and the local thermal conductivity show the percolating effect as described in the text.

Note that C does not depend on the height variable x (or z), but is simply a constant for a given ratio β of the constituent thermal conductivities. Equations 11 and 12 give an analytical expression for the temperature profile $T(x)$ for a linear concentration profile of the bad thermal conductor across the film. It is expressed in terms of the variable $x = (1-3z/d)(\beta-1)+\beta$, which varies in the range $2 - \beta < x < 2\beta - 1$ over the film thickness.

The predictions of Equation 11 are shown in Fig. 2, as well as in the second column of Table IV. Note that the drop in temperature occurs mostly in the upper (poorly-conducting) half of the film, i.e., for $z > d/2$. The drop is a strongly nonlinear function of z even though the concentration profile is linear in z. However, $T(z)$ does not drop as abruptly near $z = d$ as in the numerical simulations for the same concentration profile. Although the trend is consistent between the numerical and analytical calculations, we attribute the differences to the fact that the analytical theory is based on a simple mean-field-like estimate of the concentration profile, which overestimates how smoothly various properties vary with z.

Given the temperature profile, the effective thermal conductivity $\kappa_{e,\perp}$ perpendicular to the film can be found for any β by integrating Equation 5; the result is

$$\frac{\kappa_{e,\perp}}{\kappa_1} = \frac{3(\beta-1)}{2}\left[\ln\beta + \frac{\beta^2-1}{4\beta}\right]^{-1}. \qquad (13)$$

Thus, for $\beta = 100$, $\kappa_{e,\perp}/\kappa_1 \sim 5.0164$. This result should be compared with those shown in the second column of Table II. Similarly, $\kappa_{e,\parallel}$ can be found from Equation 7 to be $\kappa_{e,\parallel}/\kappa_1 = 35.2172$, which should be compared with the values reported in Table III. It should also be pointed out that the EMA, in its present form, does not take into account of any finite size effects [5]. The results are thus valid for films with linear dimensions, either parallel or perpendicular to the film, large compared with the grain size.

4.2.2. Quadratic concentration profile

Next we consider $p(z) = (z/d)^2$, i.e., a concentration of poor conductor which varies quadratically with height within the film. In this case, $\kappa_{e,\perp}$ can be obtained by carrying out the integration in Equation 5 numerically. For the ratio $\kappa_2/\kappa_1 = 100$ used in the network simulations of the previous section, this integration yields $\kappa_{e,\perp}/\kappa_1 = 8.79267$, significantly larger than the linear profile. The reason for this difference is that the concentration profile $(z/d)^2$, when integrated over z, gives a smaller overall volume fraction of poor conductor in the entire film than does the linear concentration profile with the same limiting concentrations. This lower overall concentration, combined with a larger concentration of good conductor at any given height within the film, leads to larger local thermal conductivities $\kappa(z)$ than in the case of a linear profile, and hence to a higher $\kappa_{e,\perp}$.

$T(z)$ for this composition profile can be obtained most conveniently by numerically integrating Equation 6. The results are shown in the third column of

Table IV. In comparison to $T(z)$ for a linear concentration profile, the temperature in the quadratic case drops more rapidly near the top (i. e., the hot) surface of the film. The reason for this behavior is that there is only a small concentration $p(z)$ of poor conductor on the cold side of the film because of its z^2 concentration-dependence. Hence, most of the film is effectively a good thermal conductor, and only a thin layer near the top surface is poorly conducting. The temperature, therefore, drops more steeply near the top surface.

We now compare the results from a linear concentration profile to those obtained from a quadratic profile containing the *same* total volume fraction of poor conductor in the entire film. The concentration profile $p(z) = [1 + 3(z/d)^2]/4$ satisfies this requirement, since $\int_0^d \frac{1}{4}[1 + 3(z/d)^2]dz = \int_0^d (z/d)dz = d/2$. Note that in this case the concentration of poor conductor at $z = 0$ is finite. This condition is needed if we require a quadratic profile distributed in such a way that $p(z = d) = 1$, while still containing the same amount of poor conductor as in a film with a linear concentration profile. The temperature profile resulting from this $p(z)$ is readily obtained numerically from Equations 2 and 6; the results are listed in the 5th column of Table IV. In comparison to the linear profile, the temperature drop is slightly steeper in the upper part of the film, because of the z^2 concentration-dependence. However, the temperature varies only slowly in the lower half of the film ($z < d/2$), because of the slow variation of the concentration of poor conductor with z in this part of the film.

4.2.3. Square-root concentration profiles

While $p(z) = (z/d)^2$ implies a smaller volume fraction of poor conductor than a linear variation, a square-root profile $p(z) = \sqrt{z/d}$ implies a *larger* volume fraction of poor conductor. In this case, the EMA leads to a thermal conductivity $\kappa_{e,\perp} = 2.99639$. This value is smaller than that of a linear profile, because of the larger amount of poor conductor. The calculated temperature profile is shown in the fourth column of Table IV. Note that $T(z)$ varies more slowly with z in the upper part of the film ($z > d/2$) than in the linear case; this slow variation is due to the relatively slow decrease in concentration of poor conductor in the upper part of the film.

Next, we consider the concentration profile $p(z) = (3/4)\sqrt{z/d}$, which carries the *same* amount of poor conductor as in a linear profile. In this case, the redistribution of poor conductor into a $\sqrt{z}$ profile leads to $p = 3/4$ at $z = d$, rather than $p = 1$ as in the linear profile. Solving for the effective thermal conductivity in this case, we find $\kappa_{e,\perp} = 12.5329$. The higher $\kappa_{e,\perp}$ results from the fact that the concentration of poor conductor is suppressed near the top of the film. In fact, $p < 3/4$ at any depth inside the film, implying that much of the film is a relatively good thermal conductor. The temperature profile for this case is shown in the 6th column of Table IV. The temperature variation is slower than in the linear case, because of the fact that $\kappa(z)$ is slowly varying with z.

The last column in Table IV gives the EMA results for $p(z) = 1 - [1 - (z/d)]^2$, the simulation results for which were shown in the last column of Table II. This profile corresponds to a concentration of good conductor which increases quadratically with distance away from the hot side ($z = d$) of the film. Qualitatively, this $p(z)$ profile looks quite similar to the square-root profile discussed earlier; hence, the temperature profile and $\kappa_{e,\perp}$ are similar to those in the fourth column of Table IV.

5. Discussion

It may appear surprising that, in dealing with a graded composite, we use a 3D rather than a 2D EMA to estimate the local thermal conductivity at a particular height z in the film. But in fact this is a correct procedure: using the 3D EMA ensures that, when the volume fraction is z-independent, the 3D EMA result is recovered.

On the other hand, the EMA procedure for a graded composite is probably most suitable only if certain geometric conditions are satisfied. We now discuss what these conditions are likely to be. Recall that the EMA is obtained (in a two-component composite, for example) by imagining a particle of each type embedded in an effective medium which is self-consistently determined. The usual EMA Equation 1 is obtained if that medium is uniform. It is reasonable to use the same procedure for a *graded* composite, therefore, if the average concentration does not vary substantially on the length scale of the size of the particles being embedded. To make this rather vague condition slightly more precise, we might demand that the volume fraction vary by no more than $|\Delta p|$ over a distance na, where Δp is a small percentage of unity, a is a typical particle radius, and $n \gg 1$ is a suitable distance factor. These conditions may be combined to give the requirement $|\mathrm{d}p/\mathrm{d}z|na < |\Delta p|$, where $\mathrm{d}p/\mathrm{d}z$ is the magnitude of the concentration gradient. Equivalently, this condition may be written

$$a|dp/dz| \ll 1. \tag{14}$$

Thus, for a *given* concentration gradient, our effective-medium approach should be best for very small particles.

The present work can be extended in a variety of ways. For example, the same numerical technique used to find the thermal conductivity within the composite in Section 3 can also be used to calculate the distribution of temperature gradients in the composite. The calculation is analogous to that used to compute the distribution of electric fields in an electrical composite. Moreover, the present approach is not limited to problems at zero frequency, nor to thermal properties. For example, one could study the optical, infrared, microwave, or nonlinear optical properties of functionally graded optical composites; these could be potentially of even greater interest than the FGC's used as thermal barriers. Finally, it might be of interest to extend the graded EMA approach used here to treat explicitly time-dependent problems, such as the time-dependent equation for thermal diffusion in the functionally graded composite.

Acknowledgements

This work has been supported by the National Science Foundation through Grant DMR 97-31511 (DS and XZ), and by the Electric Power Research Institute, Contract WO9000-35 (AJM), with special thanks to EPRI's Dr. John Stringer. PMH acknowledges the support from the Research Grants Council of the Hong Kong SAR Government through Grant CUHK4129/98P. DS acknowledges valuable conversations with E. Almaas and R. V. Kulkarni.

References

1. T. HIRAI, in "Processing of Ceramics, Part 2," edited by R. J. Brook (VCH Verlagsgesellschaft mbH, Weinheim, Germany, 1996) p. 293 and references cited therein.
2. A. J. MARKWORTH, K. S. RAMESH and W. P. PARKS, JR., *J. Mater. Sci.* **30** (1995) 2183 and references cited therein.
3. J. DERRIDA and J. VANNIMENUS, *J. Phys. A.* **15** (1982) 557.
4. E. DUERING, R. BLUMENFELD, D. J. BERGMAN, A. AHARONY and M. MURAT, *J. Stat. Phys.* **67** (1992) 113 and references cited therein.
5. X. ZHANG and D. STROUD, *Phys. Rev. B.* **52** (1995) 2131.
6. *Idem., ibid.* **49** (1994) 944.
7. For a recent review of this and other related effective-medium approximations, see, e.g., D. J. BERGMAN and D. STROUD, *Solid State Physics* **46** (1992) 178 and references cited therein.

Received 8 December 1998
and accepted 27 April 1999